Journal of Colloid and Interface Science 401 (2013) 141–147

Contents lists available at SciVerse ScienceDirect

Journal of Colloid and Interface Science

www.elsevier.com/locate/jcis

Study of colloids transport during two-phase flow using a novel polydimethylsiloxane micro-model

Qiulan Zhang [a], N.K. Karadimitriou [a], S.M. Hassanizadeh [a,b,*], P.J. Kleingeld [a], A. Imhof [c]

[a] Earth Sciences Department, Utrecht University, Budapestlaan 4, 3584 CD Utrecht, The Netherlands
[b] Soil and Groundwater Systems, Deltares, The Netherlands
[c] Soft Condensed Matter, Debye Institute, Utrecht University, 3508 TA Utrecht, The Netherlands

ARTICLE INFO

Article history:
Received 25 September 2012
Accepted 26 February 2013
Available online 7 March 2013

Keywords:
PDMS micro-model
Confocal microscopy
Fluorescent colloids
Uniform wettability
Colloid transport in two-phase flow

ABSTRACT

As a representation of a porous medium, a closed micro-fluidic device made of polydimethylsiloxane (PDMS), with uniform wettability and stable hydrophobic properties, was designed and fabricated. A flow network, with a mean pore size of 30 μm, was formed in a PDMS slab, covering an area of 1 mm × 10 mm. The PDMS slab was covered and bonded with a 120-μm-thick glass plate to seal the model. The glass plate was first spin-coated with a thin layer, roughly 10 μm, of PDMS. The micro-model was treated with silane in order to make it uniformly and stably hydrophobic. Fluorescent particles of 300 μm in diameter were used as colloids.

It is known that more removal of colloids occurs under unsaturated conditions, compared to saturated flow in soil. At the same time, the change of saturation has been observed to cause remobilization of attached colloids. The mechanisms for these phenomena are not well understood. This is the first time that a closed micro-model, made of PDMS with uniform and stable wettability, has been used in combination with confocal microscopy to study colloid transport under transient two-phase flow conditions. With confocal microscopy, the movement of fluorescent particles and flow of two liquids within the pores can be studied. One can focus at different depths within the pores and thus determine where the particles exactly are. Thus, remobilization of attached colloids by moving fluid–fluid interfaces was visualized. In order to allow for the deposition and subsequent remobilization of colloids during two-phase flow, three micro-channels for the injection of liquids with and without colloids were constructed. An outlet channel was designed where effluent concentration breakthrough curves can be quantified by measuring the fluorescence intensity. A peak concentration also indicated in the breakthrough curve with the drainage event. The acquired images and breakthrough curve successfully confirmed the utility of the combination of such a PDMS micro-model and confocal microscopy for the visualization of colloid transport in a flow network filled with two fluids, and in particular, the colloids retention, mobilization, and transport under transient flow conditions.

1. Introduction

As a representation of a porous medium, micro-models are commonly employed to study and visualize physical, chemical, and biological processes at the pore scale. During the last few decades, micro-models have proven to be a valuable tool for the study and observation of flow of fluids and transport of solutes within the pore space. They have been increasingly used to study diverse applications, such as energy-related multiphase transport in porous media [1], reservoir engineering [2], and two-phase flow experiments [3–11]. An extensive review of micro-models and their use in two-phase flow research can be found in Karadimitriou and Hassanizadeh [12], including fabrication methods, materials used, and visualization techniques.

The use of micro-chips in colloids transport is a relatively recent development. So far, mostly, an open micro-channel combined with microscopy has been used to study colloids transport [13–17], where visualization is relatively simple. But, micro-channels are too simple and in particular, various two-phase phenomena occurring in a porous medium will not occur there. One needs to have a network containing a large number of pores. Pioneering visualization experiments on colloid retention in unsaturated media were performed by Wan and Wilson [18,19] in glass micro-models under optical microscopy with fluorescent lighting system. In their system, the air phase was stagnant and water phase flowed

Abbreviations: PDMS, polydimethylsiloxane; FWI, fluorinert–water interface; SWI, PDMS–water interface; FWSC, fluorinert–water–solid contact line.

* Corresponding author at: Earth Sciences Department, Utrecht University, Budapestlaan 4, 3584 CD Utrecht, The Netherlands.
E-mail address: S.M.Hassanizadeh@uu.nl (S.M. Hassanizadeh).

0021-9797/$ - see front matter © 2013 Elsevier Inc. All rights reserved.
http://dx.doi.org/10.1016/j.jcis.2013.02.041

at steady state. Later on, etched glass micro-models were used by other research groups [20,21] to study colloids movement at pore scale with optical microscopy. They injected air bubbles into micro-models and visualized the interaction of colloids and a single air bubble under steady-state. Other materials have been also used to make micro-models for colloids transport. For example, silicon micro-models have been used to study colloids hydrodynamic behaviors in a saturated medium [22]. PDMS micro-fluidics has been used in biochemical engineering applications [23], blood micro-particles distribution [24], and multiphase/two phase flow in porous media. Compared to glass and silicon, a soft material like PDMS is more suitable for making inexpensive micro-models by rapid prototyping [25].

One of the open questions in the transport of colloids in unsaturated porous media and/or in two-phase flow is the role of fluid–fluid interfaces, as well as fluids–solid contact line, in the attachment and remobilization of colloids. Optical microscopy provides a lumped image of the whole channel depth. But, in order to investigate the interactions between colloids and fluid–fluid interfaces and/or contact lines in a two-fluid system, one needs to focus and get images at various depths within the pore space. This can be achieved with a confocal microscope. Confocal microscopy is a point-by-point visualization method. One of the fluids should either be dyed with fluorescent dyes or contain some fluorescent particles. With confocal microscopy, the sample can be tracked spatially in three dimensions by superposing two dimensional images taken at sequential z stacks [26] (z being the coordinate in the depth). Furthermore, it allows real-time information about the complex mechanisms under dynamic conditions. However, confocal microscopes have a limited depth of view. Generally, they give good results for a depth of view up to 250 μm [27]. That is the reason that mostly open micro-channels have been used in studies involving confocal microscopy; a cover plate takes up much of the depth of view and thus a very limited depth of the channel can be visualized.

In this work, we describe the design and fabrication of a closed PDMS micro-model, following a procedure described by Xia and Whitesides [28]. PDMS micro-models are very cheap to produce, and can be made under normal laboratory conditions (so, for example, a clean room is not needed). Moreover, the PDMS micro-model that we designed and manufactured had some important properties that are usually lacking in other PDMS models. First, the micro-model was made uniformly and stably hydrophobic. Second, the model was sealed with a very thin glass plate, coated with a film of PDMS. This made it possible to focus at locations throughout the whole depth of the model (30 μm). Third, the system of injection of fluids, with and without colloids, was constructed such as to avoid mixing of fluid phases at the entrance. Fourth, the inner surfaces of the pores were all PDMS. This made sure that the fluids would experience the same wetting properties everywhere; there was no mixed wettability.

To the best of our knowledge, this is the first application of PDMS micro-model combined with confocal laser scan microscopy to study the movement of fluorescent particles in a flow network. It is also the first study of colloids transport in a porous network with transient flow two immiscible liquids. Acquired images were used to analyze colloids interaction with liquid phases, water–fluorinert and liquid–solid interfaces, as well as with the fluids–solid contact lines.

2. Experimental setup, materials, and methods

2.1. Liquids and particles

As mentioned above, we were interested in generic studies of the fate of adsorbing colloidal particles under transient two-phase flow conditions. So, it is not crucial which phase is the wetting phase and which one is the non-wetting. As the two immiscible fluids, we selected deionized water and fluorinert FC-43(3M). Given the fact that our PDMS micro-model was hydrophobic, water was the non-wetting phase and fluorinert was the wetting phase. The fluorinert liquid type was chosen such that it had nearly the same index of refraction as water (1.291 and 1.332, respectively, at 20 °C). Carboxylated fluorescent microspheres (Polysciences Inc. GmbH), with an average diameter of 300 nm were used as model colloids. They were hydrophilic and weakly negatively charged at neutral pH and were labeled with fluorescein. Because we worked with large concentration of colloids (up to 10^{12} particles per liter), we had to make sure no coagulation in the colloids suspension occurred. Therefore, before injection, the colloids-water suspension was immersed in an ultrasound bath for 30 min to prevent coagulation. We were interested in colloid transport and mobilization under transient hydraulic conditions.

2.2. The flow network

A two-dimensional pore network was designed based on Delaunay triangulation. Delaunay triangulation is considered to be a good representation of a natural porous medium [29]. The network comprised an assembly of pore bodies (large pores) connected to each other by smaller pores, called pore throats. In Delaunay triangulation, points are connected to their neighbors by non-intersecting bonds. Connected points form triangles that are as equilateral as possible. The coordinates of the triangulation points were generated in MatLab. These points were considered to be the centers of the pore bodies. The network was then exported to AutoCAD sketch for further processing. An outlet channel, along with three inlet channels for the introduction of the fluids and the colloids, were added to the same sketch and connected to the network.

As can be seen in Fig. 1, the final design of the micro-model had five parts: (1) three inlet reservoirs (each 0.5 mL in volume); (2) three inlet channels (6 mm in length, 0.5 mm in width and 30 μm in depth) for introducing fluorinert, water, and water with colloid suspensions; (3) the flow network; (4) the outlet channel; (5) the outlet reservoir. The overall network dimensions were 1 mm by 10 mm, with 90 pore bodies and roughly 200 pore throats. The mean diameter of pore bodies was 30 μm. This was also the depth of all parts of the network, which was measured and found to be constant within a margin of 0.5% throughout the micro-model. The width of pore throats was between 25 μm and 30 μm. The outlet channel, as well as the outlet reservoir had some pillars (white strips) added for structural strength. Given the aspect ratio between the width and the depth of the channel and the reservoir, the top surface would collapse without the pillars [30].

2.3. Fabrication of the micro-model

Here, the fabrication of the micro-model is briefly explained. A detailed description of the procedure is given by Karadimitriou

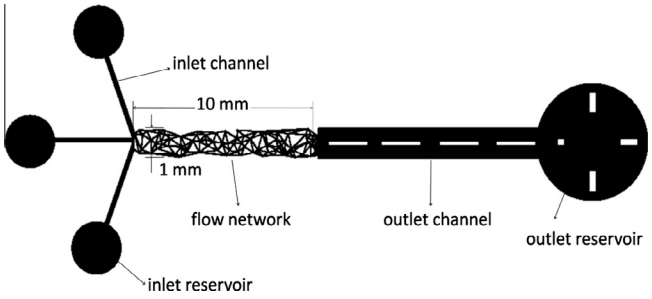

Fig. 1. Schematic representation of the micro-model (not to scale).

et al. [10]. The pore network pattern was printed on a high-resolution mask (made by CAD/Art Services, Oregon, USA). The resolution of the mask was 20,000 dpi. The mask was used to etch the flow network on a silicon wafer. This was done in a class-10,000 clean room (Kavli Institute of Nanoscience, Delft). Using the wafer, a soft-lithographic procedure was employed and the flow network with the reservoirs was formed in a PDMS slab. A 120-μm-thick glass plate from Menzel-Glaeser was then used to seal the model. The glass plate was pre-coated with a very thin layer of PDMS (less than 10 μm) with the use of a spin coater (Laurell Technologies). In this way, the phases involved in the experiments would experience the same wetting properties of the solid phase throughout the whole network. The sum of PDMS-coated glass plate thickness and the flow channel depth was kept below 250 μm. Thus, the whole channel depth was fully within the working distance of the confocal microscope. The bonding of the PDMS slide and the sealing glass slide was achieved following a corona treatment procedure. Thereafter, the model was left in an oven overnight at 68 °C to enforce bonding. An example of the constructed micro-model is shown in Fig. 2.

2.4. Silanization of the micro-model

Since PDMS is a polymeric material, its wetting properties may change with time. However, after bonding, with corona treatment, PDMS becomes hydrophilic but not stably; it degrades with time and eventually recovers its hydrophobicity. This effect starts almost immediately after exposure, and it continues until reaching the initial condition [31,32]. In order to make the wettability of the model uniform and stable, the micro-model was silanized with the use of a solution of trichloro-perfluoro-octyl-silane and 96% pure ethanol. The solution was prepared in a small air-proof beaker, and thoroughly stirred with a stirring machine. One milliliter of the solution was taken out of the beaker with a 1-ml Terumo syringe. The syringe was then put in a syringe pump, and the solution was injected into the flow network at the flow rate of 3 μL/min. We let the solution flow through the flow network for half an hour. Then, the model was put in an oven at 68 °C and was left overnight to dry out. This silanization process ensured that the micro-model became permanently and uniformly hydrophobic; even after months of use, the PDMS surface remained unchanged with time.

Given that the model was hydrophobic, water was the non-wetting phase, while fluorinert was the wetting one. The silanization process created some flakes and produced small amounts of the hydrochloric acid caused local damages to the PDMS surface. So, although PDMS surface was smooth at most places, it also had some roughness here and there. Given the fact that PDMS is highly wettable to fluorinert, it was probably covered a very thin film of fluorinert everywhere during drainage experiments. Also, rough depressions on PDMS surface were always filled by fluorinert. The film was too thin to be visible in our visualization system. Using the software *ImageJ*, the contact angle between FWI and PDMS solid surface was measured to be between 0° and 4° [33].

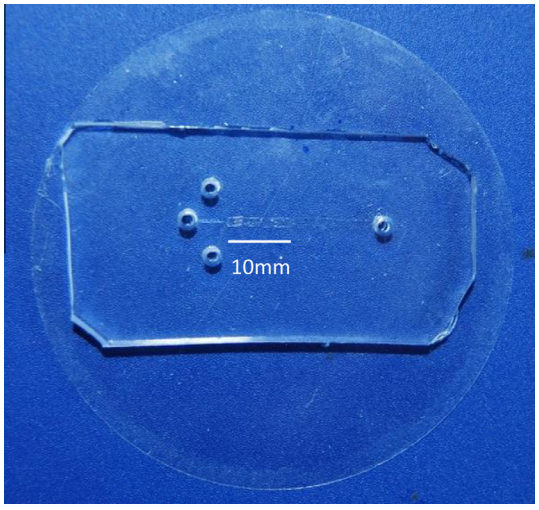

Fig. 2. Picture of the micro-model. The three inlet reservoirs, the outlet reservoir, and the flow network are visible.

2.5. Experimental setup

The experimental setup for the visualization of colloids movement (shown in Fig. 3) consisted of the following components.

2.5.1. Injection system

It comprised a dual-direction syringe pump (Harvard Apparatus GmbH), two syringes, a three-way valve, three flow-regulated reservoirs (volume 0.5 mL), and supply tubing (inner diameter of 0.15 mm). The dual-direction syringe pump could be used for both injection and withdrawal of fluids at highly-controlled small flow rates. The two syringes had volumes of 25 μL and 1 μL. The 1-μL syringe allowed us to control the flow rate in the range of 1 pL/min to 1 μL/min for displacement experiments. The bigger syringe was used for initial filling of the system with high flow rates.

In Fig. 3, we have used a color scheme to show which fluids are presented in various parts of the set-up. The three supply reservoirs were filled by fluorinert (shown in red), water (shown in blue), and colloids suspension in water (shown in green). The setup was designed such that the injection and flow regulation by the pump involved fluorinert only. So, the injection water, when needed, was achieved by injecting fluorinert into the lower part of the corresponding flow-regulated reservoir. As fluorinert is heavier than water (and colloids suspension), it pushed the water out of the reservoir and into the micro-model inflow reservoir. The fact that the pump was always operated with the same liquid meant that in needed one calibration only. So, the syringes, the three-way valve, and the lines up to the flow-regulated fluorinert reservoirs, were all filled with fluorinert at all times. Using the three-way valve, we could select the desired liquid to be injected into or withdrawn from the micro-model. The supply reservoirs ensured that the flow-regulated reservoirs always remained filled with their corresponding liquid.

2.5.2. The imaging system

It consisted of an inverted confocal laser scan microscope with oil immersion objective lens of 63× magnification (Leica TCS SP2, Heidelberg GmbH), with a numerical aperture of 1.4. We also used an oil immersion lens of 40× magnification with a numerical aperture of 1.25 during dynamic experiments. We used a 488-nm line of argon laser for excitation of fluorescent particles.

2.5.3. The PDMS micro-model

The model, described in previous section, was fixed on a support to prevent its movement under the fluid injection pressure. This assembly was placed horizontally on the stage of the microscope.

2.6. Experimental procedure

At the beginning of the experiment, the micro-model contained air only. Using the syringe pump, fluorinert was introduced into the micro-model at a constant injection rate for an extended period to expel the air and saturate the model with fluorinert. Because

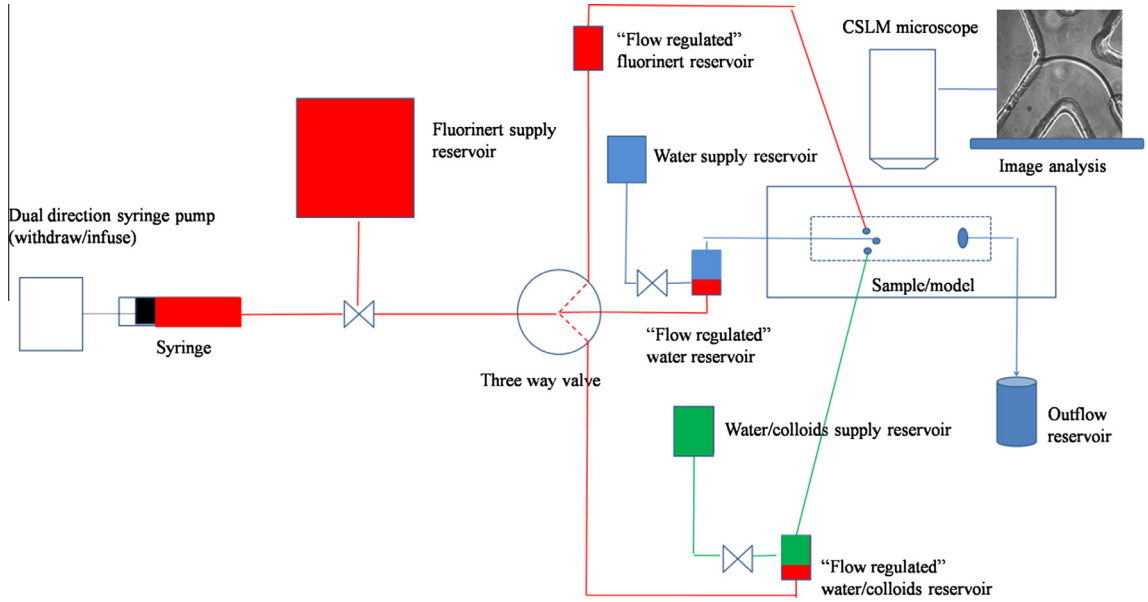

Fig. 3. Schematic of the experimental set-up. Liquids filling up various parts are shown in different colors: fluorinert in red, water in blue, water with colloids in green. (For interpretation of the references to color in this figure legend, the reader is referred to the web version of this article.)

PDMS is strongly wetting to fluorinert, air was expelled thoroughly. Nevertheless, at the start of every experiment, we checked all channels of a micro-model under microscope to ensure there is no air bubble anywhere. Then, deionized water containing colloids was injected at a constant flow rate until steady-state flow was reached. In this process, colloids-DI water suspension partially displaced the fluorinert phase to create the FWIs. After a period of injection of colloids, we switched to injecting colloids-free DI water without changing the flow rate. So, the flow remained steady state but desorption of colloids took place. The colloids adsorption and desorption was visualized during steady state flow. Also, breakthrough concentration curve in the outlet channel was measured (see Section 3). This was done by first obtained a calibration curve for colloids concentration and fluorescent intensities. Then we took real time images at the outlet channel which measured the overall volume of the whole depth. After processing the images, we calculated the concentration breakthrough curve based on the calibration curve.

To perform transient experiments, at some point during steady-state flow, we either increased the water flow rate (to cause additional drainage) or injected fluorinert (for imbibition to occur). In the experiments carried out here, the water saturation during steady-state flow was about 55–60%, and the flow rate was 50 nL/min. For transient drainage experiments, we increased the flow rate to 200 nL/min. For imbibition experiments, we injected fluorinert at the same flow rate as water was injected during steady state (namely, 50 nL/min). The total duration of a set of experiments (air expulsion, steady state flow, and transient flow) was about 3–12 h.

3. Results and discussions

3.1. Visualization of colloids retention under steady-state flow experiments

Once steady-state flow of water was established, fluorinert–water interfaces were created; images were taken focusing at various depths in different channels. A set of still images taken at one location are shown in Fig. 4. Fig. 4A was obtained by confocal microscopy in fluorescence mode, focusing at the middle of pore depth. At this step, only fluorescent particles were visualized. Then, in order to know where the particles are relative to the flow network and the FWI, the same part of the flow network was also imaged by confocal microscopy in transmission mode (i.e., optical mode). This is shown in Fig. 4B. Finally, Fig. 4C was produced by the superposition of Fig. 4A and B.

In Fig. 4B and C, parts of three pore throats and one pore body are visible. The FWI can be clearly seen. Particles were found dispersed in the water, attached to the SWI, and retained at both FWI and FWSC. No particles were found in the fluorinert, since the particles are hydrophilic. This still image only represents the behavior of the colloids at the time when the picture was taken. Even during steady-state flow, we observed relocation of attached colloids, as explained below.

Colloids did not attach to the SWIs uniformly but in the form of clusters. This is in agreement with Zevi et al. [34] who observed that particles clustered on the sand grain surfaces. This is probably due to the roughness of the solid surface (in our case created by the silanization process), where microdepressions provide favorable sites for colloids deposition [35,36]. As mentioned earlier, these depressions are most probably filled by fluorinert even in water-filled pores, such that many small-scale FWSCs are created, where colloids get attached.

In Fig. 5, we have focused on colloids accumulating at the FWSC (encircled area). Here, the accumulation is probably due to strong capillary forces at the FWI-PDMS contact line; the contact angle was measured to be less than 4°. The two images are from exactly the same domain but taken 30 min apart. The number of colloids attached to the FWSC had clearly decreased. It seemed that the mobilized colloids got reattached but some remained in water. From our real-time visualizations, we noticed a clear oscillation of the fluorinert–water meniscus. The mobilization could be due to local non-equilibrium effects induced by this oscillation. But, at this moment we have no clear explanation for it.

The experiments were repeated, and similar behaviors of particles were observed under the same conditions. Images obtained showed that the micro-model can provide clear visualization of particles retention at fluid–fluid and fluid–solid interfaces, as well as fluids–solid contact lines in steady-state two-phase flow system.

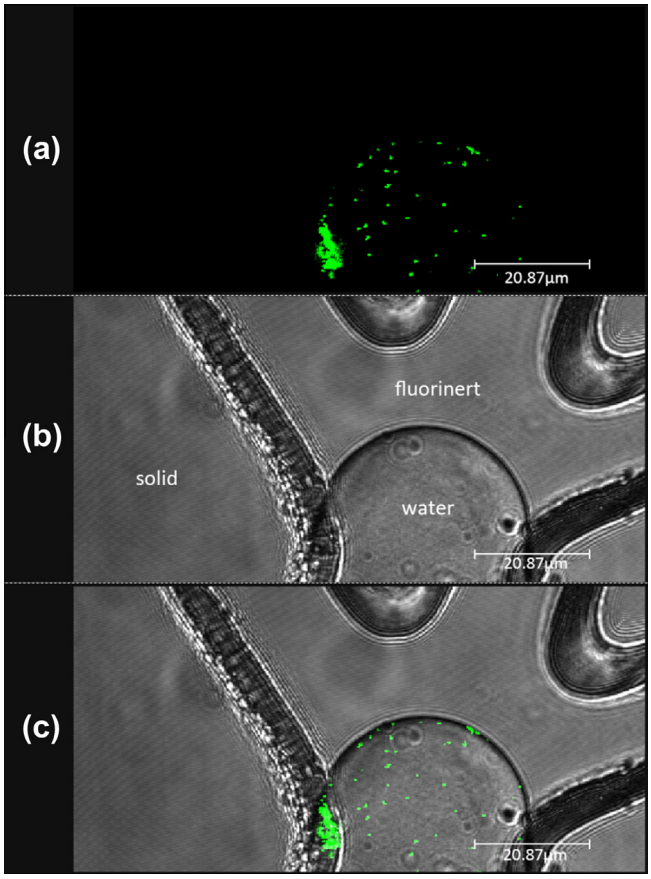

Fig. 4. Colloids retention in fluorinert and water system (images with resolution of 512 × 256 pixels). Snapshots were taken in the middle section of the micro-model. Image C is the overlaid images of A and B. Green dots are fluorescent particles. (For interpretation of the references to color in this figure legend, the reader is referred to the web version of this article.)

3.2. Visualization of colloids mobilization under transient conditions

After the deposition of colloids, the micro-model was drained; i.e. DI water (without colloids) was injected at a higher flow rate. This caused the movement of FWIs.

Real-time images were continuously captured while the moving FWI passed through our target area; see sequence of images shown in Fig. 6. Co-currently, we quantified the effluent colloids concentration breakthrough curve (as shown in Fig. 7) by measuring the fluorescent intensities at the outlet channel. These images were captured at a speed of two frames per second, with a resolution of 512 × 512 pixels per inch. The non-wetting phase (DI water) entered the imaged domain from the upper left corner. The larger pore throat A (shown in Fig. 6a) was drained first, and then the smaller pore throat B.

Fig. 6a shows the initial distribution of the colloids just before the micro-model was drained. As can be seen, a significant number of particles had been deposited on the solid surface at the junction of the two pore throats. Fig. 6b was taken 8 s later, as pore A was being invaded. Fig. 6c shows the micro-model after 20 s of interface moving, and Fig. 6d is after pore A was completely drained. The FWI moving into pore A has detached some of the adsorbed colloids. But, most colloids have remained in adsorption. Fig. 6e and f were taken while pore throat B was being drained. The majority of adsorbed colloids have been remobilized as FWI moves into pore B. Video images of these events, Movie 1 and Movie 2, are provided in the Auxiliary Materials. Remobilization of colloids led to a peak in breakthrough concentration in the outlet channel as shown in Fig. 7.

During dynamic processes, the particles were detached, and then transported with FWIs and/or the FWSC. According to Gomez-Suarez et al. [37] and Sharma et al. [38], the lower the flow rate, the more time the moving FWSCs have to dislodge attached particles. The flow rate in our experiment was of the same order of magnitude as in Sharma et al. [38], who also observed mobilization of attached particles. But, from the movies, we could observe that some colloids remained attached on the pore walls even after the passage of a FWSC. Again, this is probably due to local surface roughness, since it can provide preferential sites for the deposition of colloids [39]. This was also corroborated by Auset and Keller [40], who showed that surface roughness, may even alter the streamlines. This could be the main reason for the difference in the behaviors of the two clusters of attached particles at the entrance to the pore throat B (in Fig. 6). While the lower cluster was strongly detached and mobilized, the upper cluster detached only slightly.

4. Summary and concluding remarks

In this work, a closed micro-fluidic device made of PDMS, with uniform wettability and stable hydrophobic properties was designed and constructed. The use of this micro-model, in combination with confocal microscopy; for the study of colloids transport during two-phase flow in a porous medium was demonstrated. Water and 3M fluorinert™ FC-43 were used as two immiscible phases with nearly the same index of refraction.

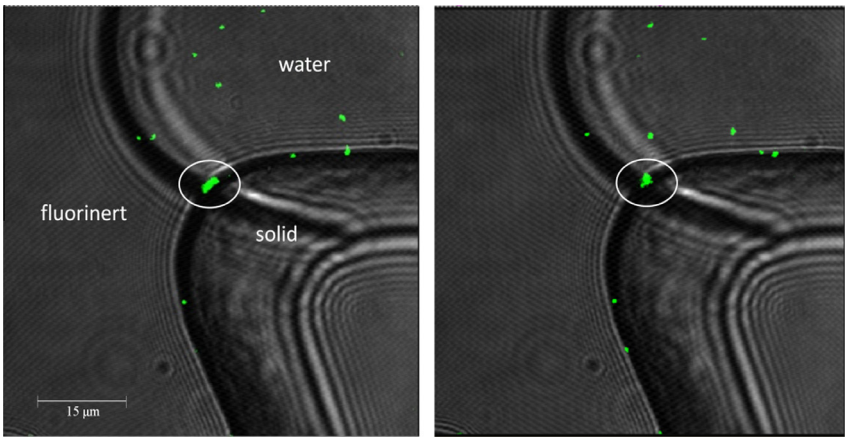

Fig. 5. Retention of colloids at FWSC. The two images are from the same location, but 30 min apart, under steady-state flow conditions.

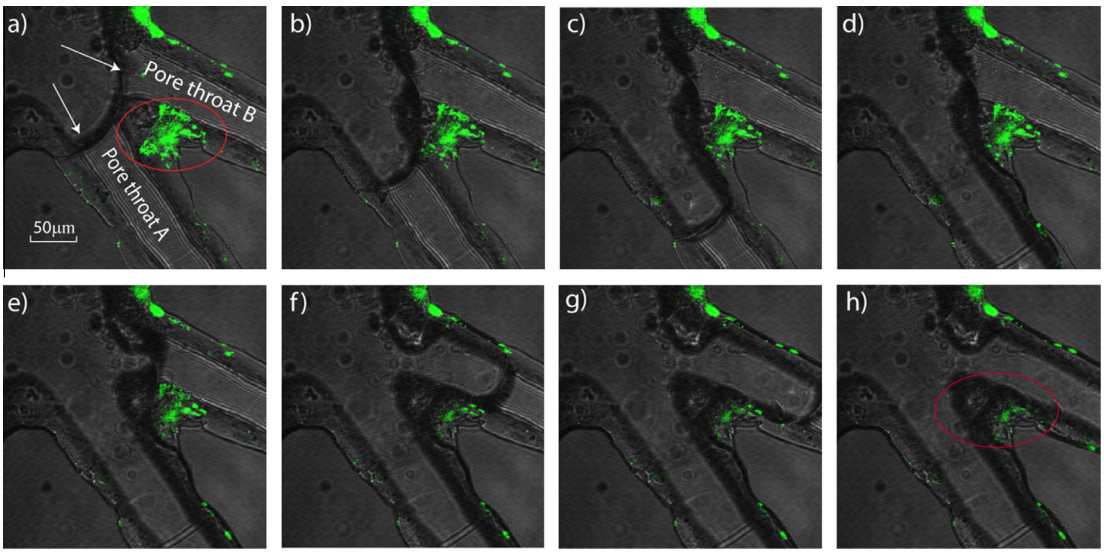

Fig. 6. Transport of colloids with the moving FWI in the micro-model. Arrows stand for the flow direction.

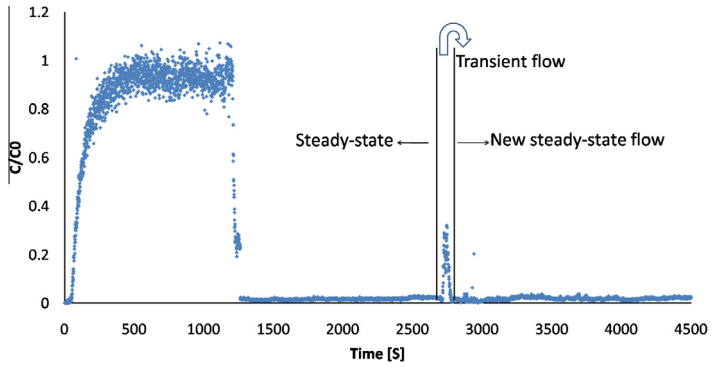

Fig. 7. Measured effluent colloid concentration breakthrough curve of the micro-model. The remobilization is due to additional drainage, where the flow rate was instantaneously increased by a factor four.

Colloids transport in the micro-model under both quasi-static and transient conditions were studied. The behavior of colloids in the micro-model was monitored with a confocal microscope. The use of transparent PDMS micro-models and confocal microscopy provides clear images at the pore scale.

The setup made it possible to perform both steady-state and transient experiments and moving of attachment/detachment of particles in partially-saturated porous media. Three separate inlet channels allowed the injection of fluids without mixing them. Colloids retention at the fluorinert–water interfaces (FWIs), water–solid interfaces (SWIs) and fluorinert–water–solid contact lines (FWSCs) were clearly visible. It was observed that FWSCs act as the major retention sites for colloids.

Under transient conditions, mobilization of deposited colloids was clearly visualized. Co-currently a concentration peak was found in the effluent breakthrough curve. The images and breakthrough curve confirm the utility of such PDMS micro-model and confocal microscopy for the study of colloids transport in porous media.

The local surface roughness of PDMS and potential presence of a thin film of fluorinert probably play an important role in the attachment of particles. But, that could not be investigated here due to limitations in visualization. Results obtained here cannot be directly applied to unsaturated soil, where colloids are in water that is the wetting phase. One needs to perform experiments where colloids can be introduced into fluorinert. Then, there would be analogy with the unsaturated soil.

Acknowledgments

We would like to acknowledge Dr. Bing Liu and Bo Peng (both from Debye Institute, Utrecht University) for training the first author on the confocal microscope. Financial support was provided by the China Scholarship Council (CSC) to the first author. The first three authors are members of the International Research Training Group NUPUS, financed by the German Research Foundation (DFG) and Netherlands Organization for Scientific Research (NWO). We are grateful to the two anonymous reviewers for their thoughtful review comments that helped to improve the manuscript significantly.

Appendix A. Supplementary data

Supplementary data associated with this article can be found, in the online version, at http://dx.doi.org/10.1016/j.jcis.2013.02.041.

References

[1] V. Berejnov, N. Djilali, D. Sinton, Lab Chip 8 (2008) 689–693.
[2] G. Naga Siva, B. Bera, N.K. Karadimitriou, S.K. Mitra, S.M. Hassanizadeh, Lab Chip (2011), http://dx.doi.org/10.1039/C1LC20556K.
[3] A. Chatenever, J.C. Calhoun Jr., AIME 195 (1952) 149–156.
[4] J.-D. Chen, D. Wilkinson, Phys. Rev. Lett. 55 (1985) 1892–1895.
[5] J. Wan, T.K. Togunaga, C.F. Tsang, G.S. Bodvarsson, Water Resour. Res. 32 (1996) 1964–1995.
[6] T. Tóth, D. Horváth, Á. Tóth, J. Chem. Phys. 127 (2007) 234506.
[7] L.-C. Chang, J.-P. Tsai, H.-Y. Shan, H.-H. Chen, Environ. Earth Sci. 59 (2009) 901–911, http://dx.doi.org/10.1007/s12665-009-0085-6.
[8] R.A. Dawe, A. Caruana, C.A. Grattoni, Transp. Porous Media (2010), http://dx.doi.org/10.1007/s11242-010-9642-4.
[9] R.A. Dawe, A. Caruana, C.A. Grattoni, Transp. Porous Media (2011), http://dx.doi.org/10.1007/s11242-010-9687-4.
[10] N.K. Karadimitriou, V. Joekar-Niasar, S.M. Hassanizadeh, P.J. Kleingeld, L.J. Pyrak-Nolte, Lab Chip (2012), http://dx.doi.org/10.1039/C2LC40530J.
[11] M. Wu, F. Xiao, R.M. Johnson-Paben, S.T. Retterer, X. Yin, K.B. Neeves, Lab Chip 12 (2012) 253–261.
[12] N.K. Karadimitriou, S.M. Hassanizadeh, Vadose Zone J., 11 (2012). http://dx.doi.org/10.2136/vzj2011.0072.
[13] V. Lazouskaya, Y. Jin, D. Or, J. Colloid Interface Sci. 303 (2006) 171–184.
[14] V. Lazouskaya, Y. Jin, Colloids Surf. A 325 (2008) 141–151.
[15] V. Lazouskaya, L.-P. Zhang, H. Gao, X. Shi, K. Czymmek, Y. Jin, Vadose Zone J. 10 (2011) 1250–1260.
[16] F. Wang, C.H. Chon, D. Li, J. Colloid Interface Sci. 352 (2010) 580–584.
[17] S. Aramrak, M. Flury, J.B. Harsh, Langmuir 27 (2011) 9985–9993.
[18] J. Wan, J.L. Wilson, Water Resour. Res. 30 (1994) 857–864.
[19] J. Wan, J.L. Wilson, Water Resour. Res. 30 (1994) 11–23.
[20] L.M. Lanning, R.M. Ford, Biotechnol. Bioeng. 78 (2002) 556–566.
[21] G. Chen, M. Flury, Eng. Aspects 256 (2005) 207–216.
[22] T. Baumann, C.J. Werth, Vadose Zone J. 3 (2004) 434–443.
[23] T. Fujii, Microelectronic Eng. (2002) 907–914.
[24] B.A. Ashcroft, J. de Sonneville, Y. Yuana, S. Osanto, R. Bertina, M.E. Kuil, T.H. Oosterkamp, Biomed. Microdev. 14 (2012) 641–649.
[25] S.R. Quake, A. Scherer, Science 290 (2000) 1536–1540.
[26] V. Prasad, D. Semwogerere, Eric R. Weeks, J. Phys. Condense.: Matter 19 (2007), http://dx.doi.org/10.1088/0953-8984/19/11/113102.
[27] J. Ekman, D. Zhang, Introductions for Leica SP2 Confocal Microscope, 2011.
[28] Y. Xia, G.M. Whitesides, Angew. Chem. Int. Ed. 37 (1998) 550–575.
[29] A. Heiba, M. Sahimi, L. Scriven, H. Davis, SPE Reserv. Eng. 7 (1992) 123–132.
[30] A. Bietsch, B. Michel, J. Appl. Phys 88 (2000) 4310–4318.
[31] J.L. Friz, M.J. Owen, J. Adhesion 54 (1995) 33–45.
[32] S.I. Murakami, T. Kuroda, Z. Osawa, J. Colloid Interface Sci. 202 (1998) 37–44.
[33] N.K. Karadimitriou, I. Xiarchos, S.M. Hassanizadeh, Appl. Surf. Sci. (2013).
[34] Y. Zevi, A. Dathe, B. Gao, W. Zhang, B.K. Richards, T.S. Steenhuis, Water Resour. Res. (2009) 45.
[35] S.A. Bradford, J. Simunek, M. Bettahar, M.T. van Genuchten, S.R. Yates, Water Resour. Res. (2006) 42.
[36] V.L. Morales, B. Gao, T.S. Steenhuis, Vadose Zone J. 8 (2009) 11–20.
[37] C. Gomez-Suarez, J. Noordmans, H.C. van der Mei, H.J. Busscher, Phys. Chem. Chem. Phys. (1999).
[38] P. Sharma, M. Flury, J. Zhou, J. Colloid Interface Sci. 326 (2008) 143–150.
[39] C. Shen, V. Lazouskaya, H. Zhang, F. Wang, B. Li, Y. Jin, Y. Huang, Colloids Surf. A: Physicochem. Eng. Aspects (2012) 98–110.
[40] M. Auset, A.A. Keller, Water Resour. Res. 42 (2006), http://dx.doi.org/10.1029/2005WR004639.